Materials Chemistry

Cite this: *J. Mater. Chem.*, 2011, **21**, 9009

www.rsc.org/materials

PAPER

Bifunctional highly fluorescent hollow porous microspheres made of $BaMoO_4 : Pr^{3+}$ nanocrystals *via* a template-free synthesis†

Xuyong Yang,[ab] Yongqin Zhou,[a] Xibin Yu,*[a] Hilmi Volkan Demir*[bcd] and Xiao Wei Sun*[be]

Received 29th January 2011, Accepted 22nd March 2011
DOI: 10.1039/c1jm10458f

We report a bifunctional hollow porous microsphere composed of single-component $BaMoO_4 : Pr^{3+}$ nanocrystals by a facile template-free synthesis. All the as-synthesized hollow microspheres are well-dispersed with a diameter of 2–4 μm and the $BaMoO_4 : Pr^{3+}$ nanocrystals measure 30–60 nm in diameter. It is observed that there are a large amount of pores with an average diameter is 17.5 nm in the shell of these $BaMoO_4 : Pr^{3+}$ hollow microspheres, thereby exhibiting a great promise for drug delivery. Meanwhile, the strong, narrow-bandwidth red emission centered at 643 nm from these nanostructures can be efficiently excited from 430 nm to 500 nm. The combination of excellent luminescent properties and a hollow porous nanostructure suggest a great promise in the application of these nanostructures in lighting and displays, and in biomedicine such as targeted drug delivery, integrated imaging, diagnosis, and therapeutics. In addition, the template-free solution synthesis can be applied to the design and fabrication of other functional architectures.

Introduction

Rare earth doped nanocrystals (NCs) have emerged as a new class of fluorescent materials, exhibiting weak light scattering and easy industrial processing compared to their macroscopic counterparts. They offer diverse applications in nanoscale electronics, solid-state lighting, displays, plastics and advanced bioanalysis.[1–8] It is well known, for instance, that the size, morphology and structure of nanomaterials significantly influence their physical and chemical properties and, therefore, their applications. In the past few decades, extensive studies have been devoted to the controlled synthesis of nanocrystals, and hollow micro/nanospheres with pores in their shells are of particular interest owing to potential applications such as in drug delivery, hydrogen storage, sensing, lightweight fillers, and catalysis, *etc.*[9–17] Recently, there is an increasing interest in the biomedical field to simultaneously construct multiple functionalities of hollow porous nanostructures, especially for the fabrication of hollow porous micro/nanospheres with fluorescent properties for targeted drug delivery, integrated imaging, diagnosis, and therapeutics applications.[18–25] For example, Wu *et al.*[18] reported multifuctional superparamagnetic fluorescent Fe_3O_4/ZnS hollow nanospheres. Shi *et al.*[21] investigated fluorescent Fe_3O_4@$mSiO_2$ hollow mesoporous structured nanocapsules for simultaneous drug delivery and cell imaging applications. However, the multifuctional hollow porous micro/nanostructures reported are not single-component and need to be further functionalized by the introduction of other components, which can cause some other serious problems, such as unstable coating of the desired materials on the surface of the hollow porous structures and the clogging of pores.[26] Therefore, the development of single-component multifunctional hollow nanostructures is very important and quite necessary.

On the other hand, various methodologies have been developed to achieve the hollow nanostructures with pores in their shells, in which self-assembly appears to be more effective for assembling the nanocrystals into two or three dimensional superstructures.[27–32] So far, the template method is one of the most common used in self-assembly to prepare hollow micro/nanospheres.[33–39] However, expensive and tedious post-treatment processes are needed, such as solvent extraction, thermal pyrolysis, or chemical etching, restricting its acceptance for practical applications.[40] Furthermore, most of self-assembly methods need to be operated at a relatively low temperature, while luminescent materials prepared at low temperature often have poor performance compared to those formed *via*

[a]*Key Lab of Rare Earth Functional Materials, Department of Chemistry, Shanghai Normal University, Shanghai, 200234, P. R. China. E-mail: xibinyu@shnu.edu.cn*
[b]*School of Electrical and Electronic Engineering, Nanyang Technological University, Nanyang Avenue, Singapore 639798. E-mail: hvdemir@ntu.edu.sg; EXWSun@ntu.edu.sg*
[c]*School of Physical and Mathematical Sciences, Nanyang Technological University, Nanyang Avenue, Singapore 639798*
[d]*Department of Electrical and Electronics Engineering, Department of Physics, UNAM–Institute of Materials Science and Nanotechnology, Bilkent University, Bilkent, Ankara, Turkey 06800*
[e]*Department of Applied Physics, College of Science, Tianjin University, Tianjin, 300072, China*
† Electronic supplementary information (ESI) available: The role of citric acid and the optimal condition for luminescence. See DOI: 10.1039/c1jm10458f

conventional solid-state reactions[41] because of their poor crystallinity. As a result, it remains a major challenge to prepare highly fluorescent hollow structures by the template-free method.

Here, we report the successful synthesis of highly fluorescent hollow porous microspheres composed of single-component $BaMoO_4 : Pr^{3+}$ nanocrystals by a solution chemistry method without any surfactant template. Ostwald ripening is responsible for the formation of the nanostructure. The solution chemistry used in this work involves homogeneous nucleation of nanocrystals with defined size and morphology, which facilitates nanocrystal assembly into two or three dimensional superstructures. In our synthetic strategy, the addition of citric acid plays a critical role in tuning the self-assembly of the hollow porous structured microspheres. Futhermore, it also inhibits the growth of $BaMoO_4$ crystals, resulting in high crystallinity nanocrystal formation. These as-synthesized nanocrystal microspheres not only present a hollow porous functional structure but also exhibit excellent luminescence properties.

Experimental

Preparation of $BaMoO_4 : Pr^{3+}$ nanocrystal hollow microspheres with porous shells

All materials were purchased from commercial sources (analytical grade) and used without further purification. The sample synthesis procedure is described as follows. First, 0.0109 g of $Pr(NO_3)_3 \cdot 6H_2O$ (99.5%), 2.4367 g of $BaCl_2$ and 2.1014 g of citric acid were added to 100 mL distilled water, which was then stirred to form a mixed solution. Second, 2.4195 g of $Na_2MoO_4 \cdot 2H_2O$ was slowly added to the mixed solution until a transparent solution was obtained. A well controlled amount of NaOH solution was then added with magnetic stirring until pH 8.5 was reached to form a white homogeneous dispersion. Subsequently, this suspension was sealed along with the mother solution in 30 mL Teflon-lined stainless steel autoclaves and then reacted at 160 °C for 4 h. Finally, the as-prepared sample was repeatedly washed with distilled water and then dried at 80 °C to yield the product.

Characterization

The structure of as-prepared products were studied using the powder X-ray diffraction (XRD) (Rigaku DMAX 2000 diffractometer equipped with Cu/Kα radiation, $\lambda = 1.5405$ Å) (40 kV, 40 mA) and transmission electron microscope (TEM, JEOL JEM-2100). The morphologies of the samples were obtained using a scanning electron microscope (SEM, JEOL, JSM-6460) and an FE-SEM (S-4800, Hitachi). The optical properties were investigated by photoluminescence (PL) and photoluminescence excitation (PLE) spectroscopy, which was carried out with a VARIAN Cary-Eclipse 500 fluorescence spectrophotometer equipped with a 60 W Xenon lamp as the excitation source. Specific surface area (S_{BET}) was calculated by the multiple-point Brunauer–Emmett–Teller (BET) method in the relative pressure range of $P/P_0 = 0.05$–1.0 by the Barrett–Joyner–Halenda (BJH) model.

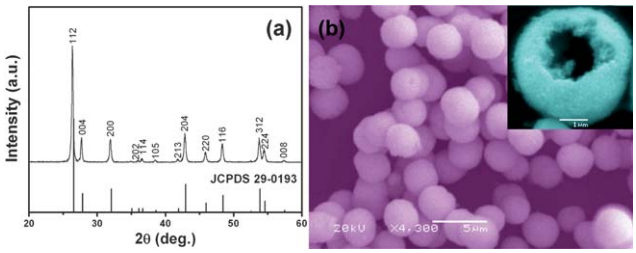

Fig. 1 (a)The XRD patterns and (b) SEM image of the $BaMoO_4 : Pr^{3+}$ hollow microspheres.

Results and discussion

A typical powder X-ray diffraction (XRD) pattern is presented in Fig. 1a. It can be observed that all of the peaks match those of scheelite-type $BaMoO_4$ (No. JCPDS 29-0193). The strong and narrow peaks indicate a high crystallinity of the as-prepared products, which is beneficial for high luminescence.[42] Scanning electron microscopy (SEM) was used to examine the morphology and grain size. All particles are spherical with a diameter of 2–4 μm (Fig. 1b). The inset SEM image in Fig. 1b clearly shows the hollow structure of these microspheres.

Careful examination of a single $BaMoO_4 : Pr^{3+}$ microsphere using field emission SEM (FESEM) (Fig. 2a) reveals that the hollow spherical structure has a rough surface and is composed of agglomerated nanocrystals. As shown in Fig. 2b, it can be seen that the nanocrystals of the hollow microsphere are well-dispersed and of 30–60 nm in diameter, which is close to that calculated by the Scherrer formula from the XRD pattern (37 nm). Fig. 2c shows a typical transmission electron microscopy (TEM) image of a single $BaMoO_4 : Pr^{3+}$ nanocrystal. It can be seen from Fig. 2d that two lattice fringes with 0.632 nm and 0.510 nm lattice spacing are identified, which are very close to the interplane spacing of the (001) and (101) planes respectively calculated from the XRD data. The corresponding selected area electron diffraction (SAED) in the inset (right) in Fig. 2d shows that the $BaMoO_4 : Pr^{3+}$ nanocrystals are essentially single crystalline in agreement with the XRD analysis.

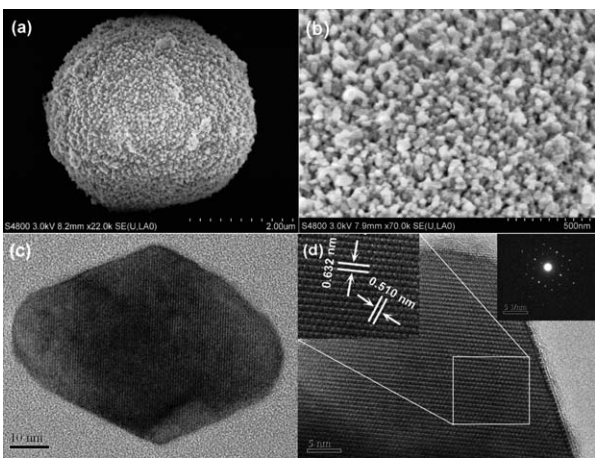

Fig. 2 (a,b) Low and high magnification FESEM images of a single hollow microsphere. (c) TEM image of a $BaMoO_4 : Pr^{3+}$ nanocrystal. (d) The corresponding HRTEM image with the selected area electron diffraction pattern.

Based on the FESEM observations, the shells of the $BaMoO_4 : Pr^{3+}$ hollow microspheres are highly porous. Nitrogen adsorption–desorption isotherms were measured to determine the specific surface area and pore volume of the $BaMoO_4 : Pr^{3+}$ hollow microspheres, and the corresponding results are presented in Fig. 3. The isotherms are typical type IV-like with a distinct H_3 hysteretic loop in the range of 0.6–1.0 P/P_0, which indicates the presence of macroporous materials according to IUPAC classification. The plot of the pore size distribution (inset in Fig. 3) was determined using the Barrett–Joyner–Halenda (BJH) method from the desorption branch of the isotherm. The average pore diameter of $BaMoO_4 : Pr^{3+}$ hollow microspheres is 17.5 nm. The Brunauer–Emmett–Teller (BET) surface area in the sample is about 18.62 $m^2\ g^{-1}$. Though this is smaller than those of mesoporous silica and carbon materials, the obtained hollow nanocrystal microspheres can be considered to have nanoporous structured walls because the metal salt compounds $BaMoO_4$ have a large density, approximately 4.65 g cm^{-3}.

In the formation of hollow porous structured microspheres, citric acid must play a key role since no other surfactants/emulsions were used. A possible formation process for these nanostructures is proposed in Fig. 4. Firstly, citric acid may form complexes with barium ions (named as BaR) to reduce the relative activity of the reactive species (Ba^{2+}) *via* van der Waals forces.[43] When NaOH is added to the reaction system, tiny crystals of $BaMoO_4$ can be formed. Meanwhile, these $BaMoO_4$ crystals are covered by the citric acid and polar carbonyl groups,[44,45] which would inhibit the further growth of the $BaMoO_4$ crystals, resulting in the formation of nanocrystals rather than bulk pieces of crystal. It is evident that citric acid can regulate the growth kinetics of $BaMoO_4$ crystals and the formation of $BaMoO_4$ microspheres (SI-1, ESI†).

Subsequently, as previous studies demonstrated, Ostwald ripening happens during the formation of the hollow microspherical structure.[46–48] The basic principle mainly explains that smaller, less crystalline or less dense particles in a colloidal aggregate will be dissolved gradually, while larger, better crystallized or denser particles in the same aggregate will grow bigger. Our time-dependent experiments agree with the above Ostwald ripening mechanism (SI-2, ESI†). Therefore, the outer, loosely packed crystallites of the solid $BaMoO_4 : Pr^{3+}$ microspheres are considered to serve as the nucleation sites for the subsequent recrystallization. In the process, as the mass was transported, the void space in the microspheres was generated mainly through Ostwald ripening. During this ripening process, the inner crystallites, which have a higher surface energy associated with their larger curvatures, would dissolve and migrate outward (purple dots), producing channels connecting the inner space and outer space in the $BaMoO_4 : Pr^{3+}$ shells.

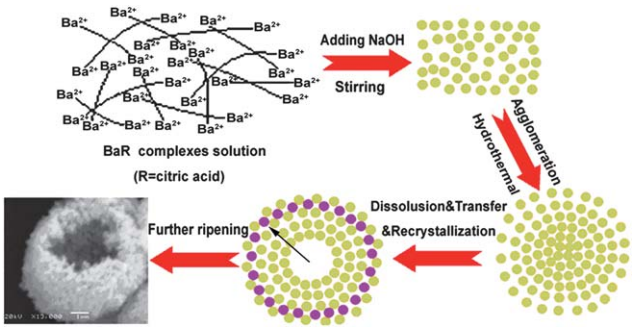

Fig. 4 Schematic illustration of the possible growth mechanism for the hollow structured $BaMoO_4 : Pr^{3+}$ microspheres. The yellow dots represent $BaMoO_4 : Pr^{3+}$ nanocrystals and the purple dots represent recrystallized $BaMoO_4 : Pr^{3+}$ nanocrystals.

The photoluminescence (PL) and PL excitation (PLE) spectra of the $BaMoO_4 : Pr^{3+}$ hollow porous microspheres are shown in Fig. 5a and the highly bright red emission excited under 365 nm lamp irradiation can be observed in the inset. A strong red emission band centered at 643 nm, which is attributed to the $^3P_0 \rightarrow {}^3F_2$ transition of Pr^{3+}, can be observed under the 450 nm excitation (Fig. 5a). The responding excitation band centered at 450 nm is attributed to $^3H_4 \rightarrow {}^3P_2$ transition. The two important factors affecting the luminescent properties of $BaMoO_4 : Pr^{3+}$ microspheres, Pr^{3+} doping concentration and crystal defects, have been discussed in detail (SI-3, ESI†). A typical energy-level diagram of PL emission for Pr^{3+} ions in $BaMoO_4 : Pr^{3+}$ samples under 450 nm excitation is described in Fig. 5b. Firstly, incident photons are absorbed by Pr^{3+} from its ground state ($^3H_4$) into the $^3P_2$ state. Then, the $^3P_2$ excited ion relaxes nonradiatively to

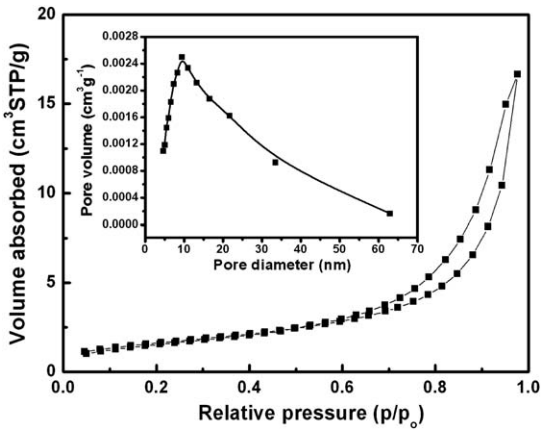

Fig. 3 N_2 absorption and desorption isotherms and pore size distributions as the inset for the as-synthesized $BaMoO_4 : Pr^{3+}$ hollow microspheres.

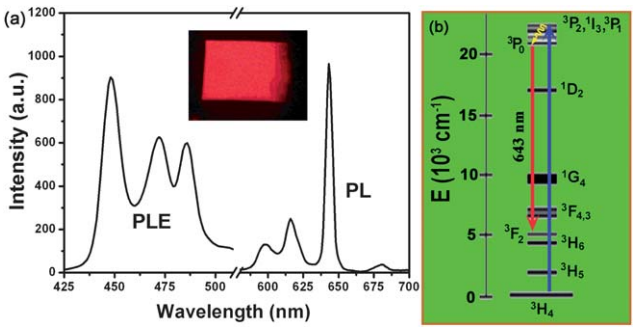

Fig. 5 (a) Luminescence spectra of $BaMoO_4 : Pr^{3+}$ microspheres, PLE (left) and PL (right). A visible luminescence photo of the sample excited under a 365 nm lamp irradiation is shown in the inset. (b) Energy-level diagram of Pr^{3+} ions in as-prepared $BaMoO_4 : Pr^{3+}$ samples.

the $^3P_0$ state and from here relaxes to the $^3F_2$ state, producing the 643nm emission band. It is noted that the $^3P_0 \rightarrow {}^3F_2$ transition of the Pr^{3+} emission linewidth is only 6 nm, which is smaller than those of typical rare earth ions (10–20 nm).[49]

Fig. 6 shows the highly luminescent emission of the as-obtained $Ba_{0.995}MoO_4 : 0.005Pr^{3+}$ sample without annealing in comparison with the commercially used red phosphor $Y_2O_2S : Eu^{3+}$ which is annealed. As shown in Fig. 6, the emission intensity of the as-synthesized $Ba_{0.995}MoO_4 : 0.005Pr^{3+}$ sample is very close to that of commercial annealed red phosphor $Y_2O_2S : Eu^{3+}$ (while the two samples are tested by the same Xenon lamp where the optical output energy of 395 nm and 450 nm lines in the Xenon lamp spectrum are very close). Generally, the emission intensity of nanoparticles without annealing process is comparatively lower because of their poorer crystallinity. For our present samples, the emission intensity is high enough without annealing for practical applications and the template-free method we used thus leads to significantly lowered energy consumption and production cost. At the same time, though sulfide phosphors such as (Ca, Sr) $S : Eu^{2+}$[50,51] and $Y_2O_2S : Eu^{3+}$[52,53] have been commercially used as red phosphors for white LEDs, their chemical stability is not desirable. Furthermore, the as-obtained red-emitting $BaMoO_4 : Pr^{3+}$ NC hollow microspheres provide the most saturated red compared to some traditional red phosphors which have been widely reported. This may be especially useful for lighting, display and advanced bioanalysis applications that require color saturation. The Commission Internationale de l'Eclairage (CIE) chromaticity coordinates of these as-obtained $BaMoO_4 : Pr^{3+}$ microspheres, $BaMoO_4 : Eu^{3+}$ red phosphor and the commercial red phosphors of $CaS : Eu^{2+}$ and $Y_2O_2S : Eu^{3+}$ are shown in the inset. The CIE chromaticity coordinates of $BaMoO_4 : Eu^{3+}$, $Y_2O_2S : Eu^{3+}$, $CaS : Eu^{2+}$ and $BaMoO_4 : Pr^{3+}$ are (0.612, 0.388),[54] (0.645, 0.354),[55] (0.670, 0.330)[56] and (0.693, 0.307), respectively. As we observed, the chromaticity point of $BaMoO_4 : Pr^{3+}$ is in the deep red region and rather close to the edge of the CIE diagram, indicating its high color purity.

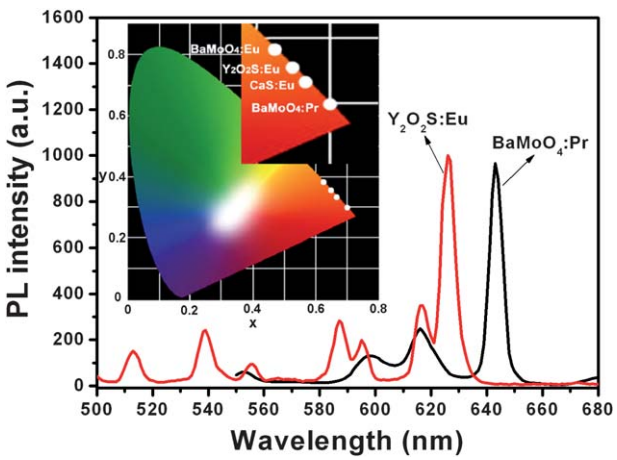

Fig. 6 PL spectra of as-obtained $Ba_{0.995}MoO_4$:0.005Pr^{3+} sample under 450 nm excitation and the commercial red phosphor $Y_2O_2S : Eu^{3+}$ under 395 nm excitation. Inset is the CIE chromaticity coordinate diagram of red-emitting $BaMoO_4 : Pr^{3+}$ microspheres compared with some traditional red phosphors.

Conclusions

In summary, the hollow porous microspheres made of $BaMoO_4 : Pr^{3+}$ nanocrystals were synthesized by a template-free solution chemistry method. High temperature annealing is not needed for the superstructures to exhibit excellent luminescence properties with high red spectral purity. Meanwhile, the combination of excellent luminescent properties of these materials and their special nanostructure may have versatile and promising applications in biomedicine. In addition, this self-assembly concept is also applicable to other compounds for the design and fabrication of novel functional architectures.

Acknowledgements

The authors would like to thank Science and Technology Development Fund (Shanghai, No. 09520500500 and No. 0752nm008), Scientific Innovation Fund of the Shanghai Education Commission (09ZZ136) and Key Laboratory of Resource Chemistry of Ministry of Education of China for supporting the research. H.V. Demir and X. Yang would also like to thank for generous support from Singapore NRF-RF-2009-09.

References

1 Henning A. Höppe, *Angew. Chem., Int. Ed.*, 2009, **48**, 3572.
2 Tsedev Ninjbadgar, Georg Garnweitner, Alexander Börger, Leonid M.Goldenberg, Oksana V. Sakhno and Joachim Stumpe, *Adv. Funct. Mater.*, 2009, **19**, 1819.
3 Yuanbing Mao, Thai Tran, Xia Guo, Jian Y. Huang, C. Ken Shih, Kang L. Wang and Jane P. Chang, *Adv. Funct. Mater.*, 2009, **19**, 748.
4 Wei Feng, Ling-Dong Sun, Ya-Wen Zhang and Chun-Hua Yan, *Small*, 2009, **5**, 2057.
5 Zhihua Li, Jinghui Zeng and Yadong Li, *Small*, 2007, **3**, 438.
6 Yiguo Su, Liping Li and Guangshe Li, *Chem. Mater.*, 2008, **20**, 6060.
7 May Nyman, Lauren E. Shea-Rohwer, James E. Martin and Paula Provencio, *Chem. Mater.*, 2009, **21**, 1536.
8 Wei-Ning Wang, W. Widiyastuti, Takashi Ogi, I. Wuled Lenggoro and Kikuo Okuyama, *Chem. Mater.*, 2007, **19**, 1723.
9 Xiaoqing Huang, Huihui Zhang, Changyou Guo, Zhiyou Zhou and Nanfeng Zheng, *Angew. Chem., Int. Ed.*, 2009, **48**, 4808.
10 Haolan Xu and Wenzhong Wang, *Angew. Chem., Int. Ed.*, 2007, **46**, 1489.
11 Sheng Peng and Shouheng Sun, *Angew. Chem., Int. Ed.*, 2007, **46**, 4155.
12 Marcos Sanles-Sobrido, Wibke Exner, Laura Rodríguez-Lorenzo, Benito Rodríguez-González, Miguel A. Correa-Duarte, Ramon A. Álvarez-Puebla and Luis M. Liz-Marzán, *J. Am. Chem. Soc.*, 2009, **131**, 2699.
13 Yu Chen, Hangrong Chen, Limin Guo, Qianjun He, Feng Chen, Jian Zhou, Jingwei Feng and Jianlin Shi, *ACS Nano*, 2010, **4**, 529.
14 Dianyan Li, Zhichao Guan, Wenhua Zhang, Xi Zhou, Wei Yun Zhang, Zhixia Zhuang, Xiaoru Wang and Chaoyong James Yang, *ACS Appl. Mater. Interfaces*, 2010, **2**, 2711.
15 Ying Chen, Xianchuang Zheng, Hanqing Qian, Zhiqing Mao, Dan Ding and Xiqun Jiang, *ACS Appl. Mater. Interfaces*, 2010, **2**, 3532.
16 Yufang Zhu, Toshiyuki Ikoma, Nobutaka Hanagata and Stefan Kaskel, *Small*, 2010, **6**, 471.
17 Jiaguo Yu, Wen Liu and Huogen Yu, *Cryst. Growth Des.*, 2008, **8**, 930.
18 Zhenxuan Wang, Limin Wu, Min Chen and Shuxue Zhou, *J. Am. Chem. Soc.*, 2009, **131**, 11276.
19 Sarit S. Agasti, Apiwat Chompoosor, Chang-Cheng You, Partha Ghosh, Chae Kyu Kim and Vincent M. Rotello, *J. Am. Chem. Soc.*, 2009, **131**, 5728.

20 Guohui Wu, Alexander Mikhailovsky, Htet A. Khant, Caroline Fu, Wah Chiu and Joseph A. Zasadzinski, *J. Am. Chem. Soc.*, 2008, **130**, 8175.
21 Yu Chen, Hangrong Chen, Deping Zeng, Yunbo Tian, Feng Chen, Jingwei Feng and Jianlin Shi, *ACS Nano*, 2010, **4**, 6001.
22 Fan Zhang, Yifeng Shi, Xiaohong Sun, Dongyuan Zhao and Galen D. Stucky, *Chem. Mater.*, 2009, **21**, 5237.
23 Guang Jia, Hongpeng You, Yanhua Song, Yeju Huang, Mei Yang and Hongjie Zhang, *Inorg. Chem.*, 2010, **49**, 7721.
24 Guang Jia, Hongpeng You, Kai Liu, Yuhua Zheng, Ning Guo and Hongjie Zhang, *Langmuir*, 2010, **26**, 5122.
25 Hai-Sheng Qian, Yong Hu, Zheng-Quan Li, Xing-Yun Yang, Liang-Chao Li, Xian-Ting Zhang and Rong Xu, *J. Phys. Chem. C*, 2010, **114**, 17455.
26 X. Lou and L. A. Archer, *Adv. Mater.*, 2008, **20**, 1853.
27 Fan Zhang, Gary B. Braun, Yifeng Shi, Yichi Zhang, Xiaohong Sun, Norbert O. Reich, Dongyuan Zhao and Galen Stucky, *J. Am. Chem. Soc.*, 2010, **132**, 2850.
28 Yufang Zhu, Toshiyuki Ikoma, Nobutaka Hanagata and Stefan Kaskel, *Small*, 2010, **6**, 471.
29 Wei Feng, Ling-Dong Sun, Ya-Wen Zhang and Chun-Hua Yan, *Small*, 2009, **5**, 2057.
30 Penghe Qiu and Chuanbin Mao, *ACS Nano*, 2010, **4**, 1573.
31 Sung-Wook Kim, Tae Hee Han, Jongsoon Kim, Hyeokjo Gwon, Hyoung-Seok Moon, Sang-Won Kang, Sang Ouk Kim and Kisuk Kang, *ACS Nano*, 2009, **3**, 1085.
32 Andrew M. Collins, Christine Spickermann and Stephen Mann, *J. Mater. Chem.*, 2003, **13**, 1112.
33 Xue-Jun Wu and Dongsheng Xu, *J. Am. Chem. Soc.*, 2009, **131**, 2774.
34 H. Djojoputro, X. F. Zhou, S. Z. Qiao, L. Z. Wang, C. Z. Yu and G. Q. Lu, *J. Am. Chem. Soc.*, 2006, **128**, 6320.
35 Qunhui Sun and Yulin Deng, *J. Am. Chem. Soc.*, 2005, **127**, 8274.
36 Dongyeon Son, Alejandro Wolosiuk and Paul V. Braun, *Chem. Mater.*, 2009, **21**, 628.
37 Yang Zhang, Meihua Yu, Liang Zhou, Xufeng Zhou, Qingfei Zhao, Hexing Li and Chengzhong Yu, *Chem. Mater.*, 2008, **20**, 6238.
38 Hélène Blas, Maud Save, Pamela Pasetto, Cédric Boissière, Clément Sanchez and Bernadette Charleux, *Langmuir*, 2008, **24**, 13132.
39 Bing Tan and Stephen E. Rankin, *Langmuir*, 2005, **21**, 8180.
40 Ye Jin, Jiahua Zhang, Shaozhe Lu, Haifeng Zhao, Xia Zhang and Xiaojun Wang, *J. Phys. Chem. C*, 2008, **112**, 5860.
41 W. B., S. Brinkley, J. Hu, A. Mikhailovsky, S. P. DenBaars and R. Seshadri, *Chem. Mater.*, 2010, **22**, 2842.
42 Xuyong Yang, Jie Liu, Hong Yang, Xibin Yu, Yuzhu Guo, Yongqin Zhou and Jieyu Liu, *J. Mater. Chem.*, 2009, **19**, 3771.
43 Yiguo Su, Liping Li and Guangshe Li, *Chem. Commun.*, 2008, 4004.
44 Jianhui Zhang, Huaiyong Liu, Zhenlin Wang, Naiben Ming, Zhongrui Li and Alexandru S. Biris, *Adv. Funct. Mater.*, 2007, **17**, 3897.
45 K. X. Yao and H. C. Zeng, *J. Phys. Chem. C*, 2007, **111**, 13301.
46 Hua Gui Yang and Hua Chun Zeng, *J. Phys. Chem. B*, 2004, **108**, 3492.
47 Jia Hong Pan, Xiwang Zhang, Alan Jianhong Du, Darren D. Sun and James O. Leckie, *J. Am. Chem. Soc.*, 2008, **130**, 11256.
48 Xiaochuan Duan, Jiabiao Lian, Jianmin Ma, Tongil Kim and Wenjun Zheng, *Cryst. Growth Des.*, 2010, **10**, 4449.
49 Li Li, Chia-Kuang Tsung, Zhi Yang, Galen D. Stucky, Lingdong Sun, Jianfang Wang and Chunhua Yan, *Adv. Mater.*, 2008, **20**, 903.
50 Y. Hua, W. Zhuang, H. Ye and S. Zhang, *J. Lumin.*, 2005, **111**, 139.
51 I. W. Park, J. H. Kim, J. S. Yoo, H. H. Shin, C. K. Kim and C. K. Choi, *J. Electrochem. Soc.*, 2008, **155**, J132.
52 F. M. Pontes, M. A. M. A. Maurera, A. G. Souza, E. Longo, E. R. Leite, R. Magnani, M. A. C. Machado, P. S. Pizani and J. A. Varela, *J. Eur. Ceram. Soc.*, 2003, **23**, 3001.
53 J. Thirumalai, R. Jagannathan and D. C. Trivedi, *J. Lumin.*, 2007, **126**, 353.
54 Yongqin Zhou, Jie Liu, Xuyong Yang, Xibin Yu and Jie zhuang, *J. Electrochem. Soc.*, 2009, **157**, H278.
55 Li-Ya Zhou, Jian-She Wei, Ling-Hong Yi, Fu-Zhong Gong, Jun-Li Huang and Wei Wang, *Mater. Res. Bull.*, 2009, **44**, 1411.
56 H. Takashima, K. Shimada, N. Miura, T. Katsumata, Y. Inaguma, K. Ueda and M. Itoh, *Adv. Mater.*, 2009, **21**, 3699.